Flight condition 2:

$$P_2(s) = \left.\frac{q(s)}{\delta_e(s)}\right|_{\text{FC2}} = \frac{-36.269(s+1.554)}{(s+4.904)(s-1.784)} \tag{7}$$

Flight condition 3:

$$P_3(s) = \left.\frac{q(s)}{\delta_e(s)}\right|_{\text{FC3}} = \frac{-11.308(s+0.637)}{(s+1.878)(s-0.560)} \tag{8}$$

Flight condition 4:

$$P_4(s) = \left.\frac{q(s)}{\delta_e(s)}\right|_{\text{FC4}} = \frac{-12.320(s+0.821)}{(s+1.923)(s-0.640)} \tag{9}$$

Here we take the average value of poles, zeros, and steady-state gains of these flight conditions as the nominal plant

$$P_0(s) = \frac{-19.576(s+0.974)}{(s+2.943)(s-1.053)} \tag{10}$$

For model reference self-organizing fuzzy logic control, we need to establish an adequate reference model for the learning supervisor. Using Ref. 8, the reference model is chosen as

$$T_m(s) = \frac{6.036(s+7)}{s^2+11.7s+42.25} \tag{11}$$

which yields 0.69-s peak time and 0.76% maximum overshoot. The unit-step response of this reference model is shown in Fig. 2, which justifies the desired time response.

By applying the proposed self-organizing fuzzy logic control to the nominal plant, the step responses of the training process are given in Fig. 3, which shows that even if the plant is unstable, the training process can stabilize the system and achieve the convergence of the system performance to the reference model. By applying the learned fuzzy control rules to the F-4E flight system control, the control performance is demonstrated in Fig. 2, which shows that the MR-SOFC design method can achieve satisfactory performance and robustness when the flight system is subjected to plant variations arising from different flight conditions.

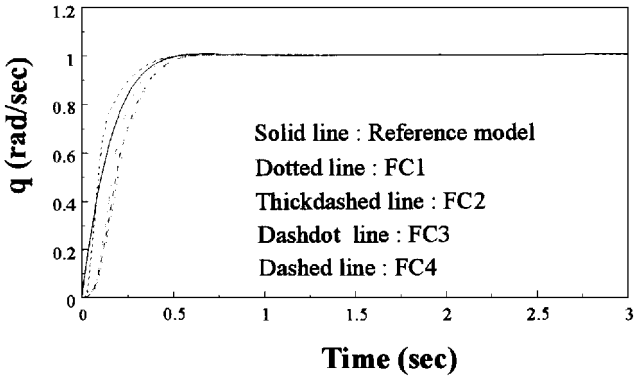

Fig. 2 Step responses of F-4E flight system for different flight conditions; command input q_c = 1 rad/s.

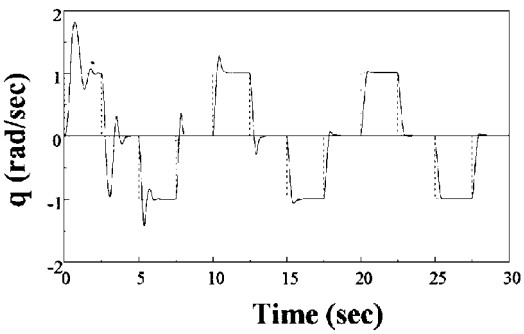

Fig. 3 Step responses of the training process.

Conclusion

The design method of MR-SOFC is proposed. By using this design method, a fuzzy rule base is learned to control the F-4E flight system. The simulations indicate that the proposed self-organizing fuzzy logic flight control can achieve satisfactory performance and robustness with respect to plant variations arising from different flight conditions.

Acknowledgments

This work was supported by the National Science Council of the Republic of China under Grant NSC86-2213-E-155-028. The authors are grateful to the reviewers and to the Associate Editor for their valuable comments and suggestions.

References

[1] Mamdani, E. H., "Application of Fuzzy Algorithms for Simple Dynamic Plant," *IEE Proceedings-D*, Vol. 121, No. 12, 1974, pp. 1585–1588.

[2] Sugeno, M. (ed.), *Industrial Applications of Fuzzy Control*, Elsevier Science, Amsterdam, 1985.

[3] Tagkagi, T., and Sugeno, M., "Fuzzy Identification of System and Its Applications to Modeling and Control," *IEEE Transactions on System, Man and Cybernetic*, Vol. 15, No. 1, 1985, pp. 116–132.

[4] Zimmermann, H. J., *Fuzzy Set Theory and Its Application*, 2nd ed., Kluwer Academic, Boston, MA, 1991.

[5] Procyk, T. J., and Mamdani, E. H., "A Linguistic Self-Organizing Process Controller," *Automatica*, Vol. 13, No. 1, 1979, pp. 15–30.

[6] Zhang, B. S., and Edmunds, J. M., "Self-Organizing Fuzzy Logic Controller," *IEE Proceedings-D*, Vol. 139, No. 5, 1992, pp. 460–464.

[7] Franklin, S. N., and Ackermann, J., "Robust Flight Control: A Design Example," *Journal of Guidance and Control*, Vol. 4, No. 6, 1981, pp. 579–605.

[8] Lin, C. M., and Shi, Z. R., "Quantitative Performance Robustness Linear Quadratic Optimal System Design," *Journal of Guidance, Control, and Dynamics*, Vol. 19, No. 3, 1996, pp. 600–604.

Minimum Drag Control Allocation

Wayne C. Durham,* John G. Bolling,† and Kenneth A. Bordignon†
Virginia Polytechnic Institute and State University, Blacksburg, Virginia 24061

Introduction

IN Ref. 1, we described a method of control allocation based on the instantaneous rate limits of the control effectors. The chief drawback to this method was the fact that the current positions were dependent on the path (in moment space) followed and would generally result in nonzero deflections in response to zero moment demands. The problem was alleviated by continuously applying unused rate capabilities to drive the solution toward one with the desired characteristics via the null space of the control effectiveness matrix.

We have long advocated the idea of including forces as well as moments in the effects of the controls[2] that would, among other benefits, permit the determination of minimum control generated drag during cruise or maneuvering. Thus, to include just drag, we have not the three-dimensional attainable moment subset (ΔAMS), but the four-dimensional attainable objective subset (ΔAOS), whose coordinates are the three moments plus drag. The moments required of the control effectors are determined by the control law and may be considered to be specified. Because we are in the ΔAOS we

Received May 20, 1996; revision received Sept. 22, 1996; accepted for publication Sept. 23, 1996.

* Associate Professor, Aerospace and Ocean Engineering Department, 215 Randolph Hall. Senior Member AIAA.

† Graduate Assistant, Aerospace and Ocean Engineering Department, 215 Randolph Hall.

actually calculate specified changes in desired moments. The actual change in drag, however, is not specified but is to be chosen as the greatest negative value attainable. Thus, the allocation problem is not to find controls that generate four specified objectives, but that generate three of those objectives and minimize the fourth.

Method

The methods previously described as direct allocation[2,3] may be easily modified to solve the problem of specifying three objectives and minimizing the fourth. In the current discussion, the objectives are the changes ΔC_l, ΔC_m, ΔC_n, and ΔC_D, and the admissible controls are those that lie within the specified constraints, $\Delta \boldsymbol{u}_{\min}$ and $\Delta \boldsymbol{u}_{\max}$. Define the vector

$$\Delta \boldsymbol{C} = \{\Delta C_l, \Delta C_m, \Delta C_n, \Delta C_D\}^T \tag{1}$$

To begin this discussion, assume the desired objectives are specified as $\Delta \boldsymbol{C}_d = \{0\ 0\ 0\ -1\}^T$. Then direct allocation will first calculate the intersection of this vector with the ΔAOS. If the scaling step is omitted, then the solution is on the boundary of the ΔAOS and the answers returned by this algorithm, $\Delta \boldsymbol{u}$, are those that result in no change in any moment coefficient but that result in the greatest negative change in drag coefficient. The $\Delta \boldsymbol{u}$ will be limited by the more restrictive of the rate or position limits of the controls' ability to travel in one computational frame; assuming the latter is the more restrictive, then the controls will move at their maximum rate toward the condition of minimum drag configuration.

The vector $\{0\ 0\ 0\ -1\}^T$ does not satisfy an arbitrary demand for desired moment coefficients ΔC_l, ΔC_m, and ΔC_n, nor does the intersection of the vector $\{\Delta C_l\ \ \Delta C_m\ \ \Delta C_n\ \ -1\}^T$ with the ΔAOS represent the desired condition because all four components will be scaled to the boundary. What is required is a method that first calculates the $\Delta \boldsymbol{u}$ that yields ΔC_l, ΔC_m, and ΔC_n, for arbitrary (unspecified) ΔC_D, and beginning from this solution, moves in the direction of minimum drag. The first step is the simple three-moment problem, and the second is solved by relocating the origin of the ΔAOS to this solution and then allocating a further $\Delta \boldsymbol{u}'$ for the vector $\{0\ 0\ 0\ -1\}^T$. That is, 1) solve the three-moment problem from

$$\Delta \boldsymbol{m} = \boldsymbol{B}_{3\times m}\Delta \boldsymbol{u}; \qquad \Delta \boldsymbol{m} = \{\Delta C_l \Delta C_m \Delta C_n\}^T \tag{2}$$

for $\Delta \boldsymbol{u}$ subject to $\Delta \boldsymbol{u}_{\min} \le \Delta \boldsymbol{u} \le \Delta \boldsymbol{u}_{\max}$, 2) move the origin such that

$$\Delta \boldsymbol{u}'_{\min} = \Delta \boldsymbol{u}_{\min} - \Delta \boldsymbol{u} \tag{3}$$

$$\Delta \boldsymbol{u}'_{\max} = \Delta \boldsymbol{u}_{\max} - \Delta \boldsymbol{u} \tag{4}$$

and 3) solve the four-objective problem on the boundary of the ΔAOS from

$$\Delta \boldsymbol{C}_d = \boldsymbol{B}_{4\times m}\Delta \boldsymbol{u}'; \qquad \Delta \boldsymbol{C}_d = \{0\quad 0\quad 0\quad -1\}^T \tag{5}$$

for $\Delta \boldsymbol{u}'$ subject to $\Delta \boldsymbol{u}'_{\min} \le \Delta \boldsymbol{u}' \le \Delta \boldsymbol{u}'_{\max}$. Following these calculations, we have

$$\boldsymbol{u}_{k+1} = \boldsymbol{u}_k + \Delta \boldsymbol{u} + \Delta \boldsymbol{u}' \tag{6}$$

The increment $\Delta \boldsymbol{u}$ satisfies Eq. (2), and the increment $\Delta \boldsymbol{u}'$ holds $\Delta \boldsymbol{m}$ fixed and moves toward minimum drag.

The algorithm as presented does not purport to converge to the minimum drag solution (i.e., it does not iterate in a given frame). Rather, it takes single steps toward that solution based on local slopes. Because the minimum drag solution is dynamically varying as the airplane maneuvers, it would not make sense to spend too much effort finding a converged solution that may be obsolete in the next frame. On the other hand, if the minimum drag solution is not varying rapidly, then we would like ultimately to converge to that solution.

The nature of drag effectiveness of several controls leads to slope reversals in the controls' drag effectiveness about their minimum drag deflections and may cause the solution to oscillate about those deflections. Whether it does or not depends on whether the frame limits are suitably small and on how well the drag effectiveness is modeled. In the implementation to be described, the user was able to select a scaling constant c_s that ranged from 0 to 1 to be used in adjusting the increment $\Delta \boldsymbol{u}'$ in Eq. (6) so that

$$\boldsymbol{u}_{k+1} = \boldsymbol{u}_k + \Delta \boldsymbol{u} + c_s \Delta \boldsymbol{u}' \tag{7}$$

Values $0 < c_s < 1$ provided convergence for unchanging minimum drag solutions at the expense of achieving less than minimum drag during dynamic maneuvers.

Example

The drag-minimizing allocation scheme just described was implemented in a fully nonlinear F-18 simulation. The basic simulation architecture was taken from Ref. 4. The F-18 model did not incorporate existing F-18 flight control laws nor the logic to prioritize and distribute commands to the control surfaces. To have a basis for comparison for the minimum drag allocation method, a second version of the simulation was developed that had the same rate limiting allocation scheme with the exception that a simple three moment pseudoinverse solution was used to restore the controls via the null space of the control effectiveness matrix. Other simulation details were as follows.

1) The five control effectors used for allocation were left horizontal tail, right horizontal tail, left aileron, right aileron, and combined rudders. The position limits used were +10.5, −24.0 deg for the horizontal tails, ±25 deg for the ailerons, and ±30 deg for the rudders. First-order actuator models were implemented with time constants of 0.05 s and rate limits of 40, 100, and 56 deg/s for the horizontal tails, ailerons, and rudders, respectively.

2) Reference 4 provides static trim subroutines that were used to initialize the simulation prior to each run. Because the control allocation methods used were based on framewise deflection limits related to the actuator rate capabilities, these methods could not be used for trimming statically. For trimming, therefore, global control position limits were used based on local control moment effectiveness data. Drag influences were not included. With the exception of local effectiveness data, this allocation method is identical to that described in Ref. 2.

3) To provide moment commands to the allocator, a simple nonlinear dynamic inversion control law was implemented. The inputs to the control law were angle-of-attack command (longitudinal stick), body axis roll rate command (lateral stick), and sideslip command (pedals). Simulations were flown in batch mode with time histories of pilot inputs provided by a maneuver generator.

4) The frame length of the simulation was 0.05 s, equivalent to an update rate of 20 Hz. The control effectiveness matrix was updated, and the control allocation subroutines were invoked, once in each frame. This made the maximum frame limits ±2 deg for the horizontal tails, ±5 deg for the ailerons, and ±2.8 deg for the rudders.

5) For the purpose of comparing the drag performance of two separate control allocation schemes, it is desirable to have the change in drag coefficient result from a change in drag only. Therefore, a simple autothrottle was implemented into the control law. This was done to dampen the phugoid mode (which was excited in the minimum drag allocation) and to hold a constant reference velocity. In addition, the air data computer from Ref. 4 was modified so that density was independent of the altitude.

6) The scaling constant c_s used to restore the controls in Eq. (7) was set at 0.1 for this simulation. This value was chosen so that the rate of convergence would be rather slow, allowing for a better analysis of the minimum drag restoring process. For general usage, this constant would be tailored for the task at hand, taking into account the tradeoffs between speed of convergence and control oscillations that occur near their minimum drag positions.

Results and Discussion

All results presented were begun from straight, symmetric, level, trimmed flight at 4-deg angle of attack and an altitude of 10,000 ft, with a true airspeed of 495 ft/s. From this flight condition, a multiaxis maneuver was performed. The multiaxis maneuver consisted of a ramp input in angle of attack (α) from 4 (trim) to 6 deg in 4 s beginning at $t = 3$ s, ending and returning to trim at $t = 7$ s; one-half cycle of a sinusoidal sideslip (β) command between 5 and 15 s, $\beta = -4\sin[\pi(t-5)/10]$ deg, $5 \le t \le 15$ s; and one full cycle of

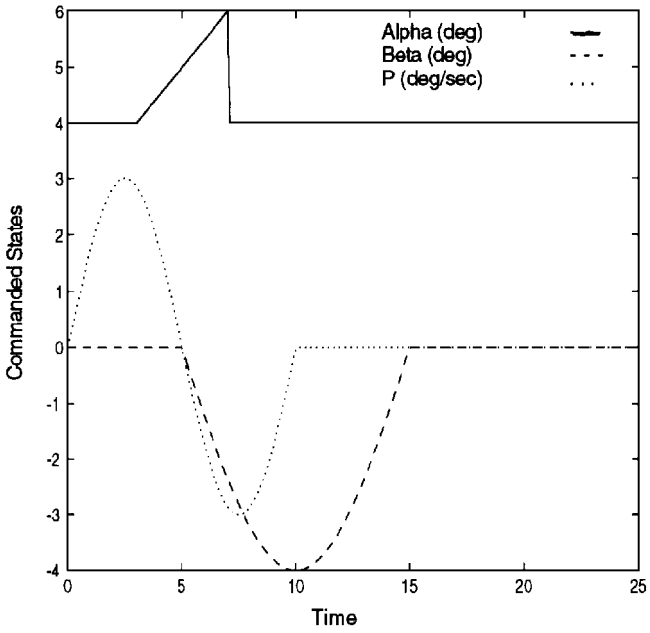

Fig. 1 Maneuver generator commands.

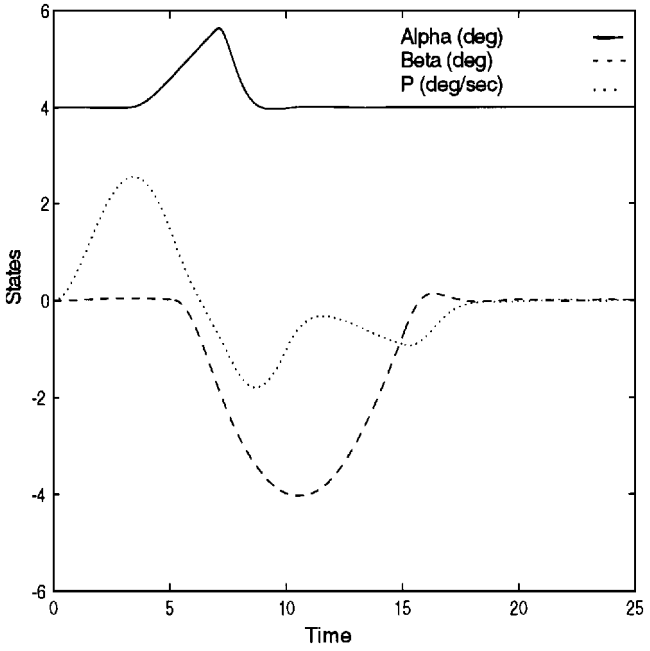

Fig. 2 Aircraft states with minimum drag allocation.

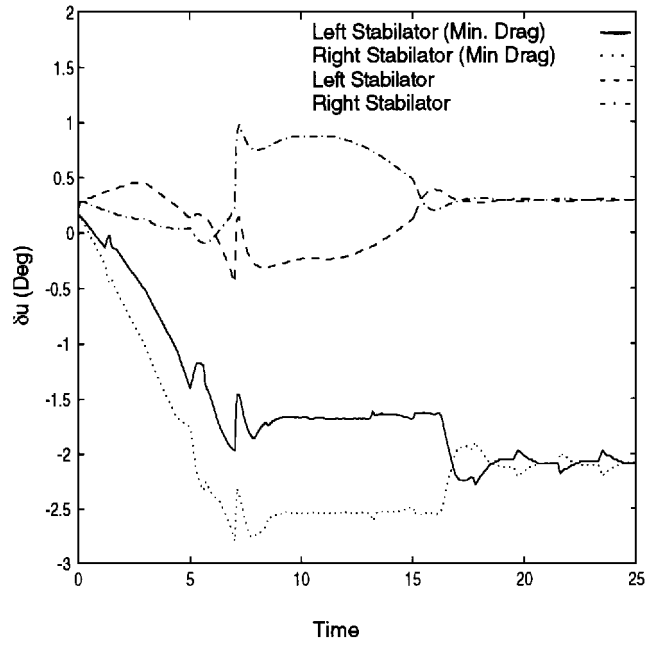

Fig. 3 Horizontal tail time histories.

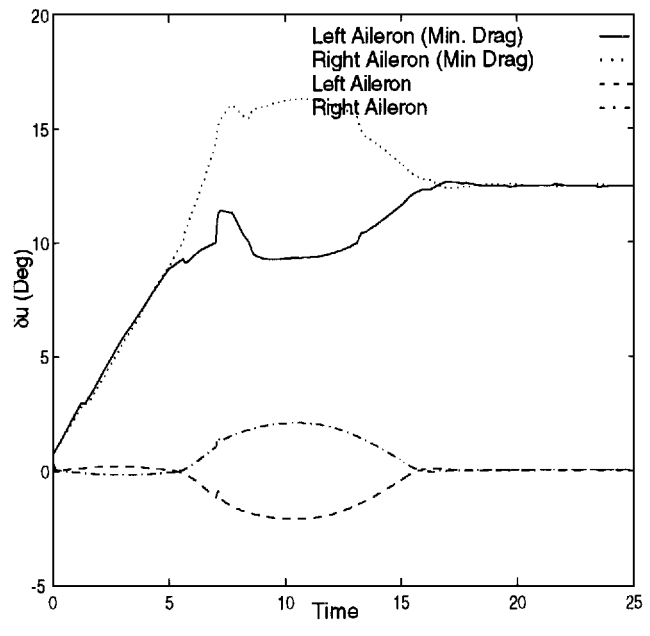

Fig. 4 Aileron time histories.

sinusoidal roll rate (p) command ending in 10 s, $p = 3\sin[\pi t/5]$ deg/s, $0 \leq t \leq 10$ s. Time histories of these commanded inputs are shown in Fig. 1.

Because the trimmed control positions were obtained using different rules, both allocation schemes (restoring to minimum drag and restoring to the pseudoinverse) began reconfiguring the control positions as the simulation was started. In performing the maneuver depicted in Fig. 1, both allocation schemes delivered control deflections that resulted in nearly identical time histories of the commanded variables. Because of space constraints, however, only the commanded states for the minimum drag allocation are shown (Fig. 2).

By definition, the pseudoinverse yields the minimum norm of the vector of control deflections. If in fact the minimum drag solution is related to zero deflections, then the pseudoinverse solution should produce fairly low-drag control deflection time histories. Figure 3 shows the horizontal tail deflections for the pseudoinverse restoring and minimum-drag restoring simulations. The aileron time histories are depicted in Fig. 4. As expected, the pseudoinverse restoring uses small deflections throughout the maneuver. The minimum drag restoring, however, allocates deflections that are significantly larger in magnitude. Loosely, the minimum drag solution finds the tradeoff between the pitching moment capabilities and drag characteristics of the ailerons and the horizontal tails, as it deflects the high-drag horizontal tails to their minimum drag positions, and then deflects the ailerons down to cancel the additional nose-up pitching moment produced.

Figure 5 shows the average rudder deflections for the pseudoinverse and minimum drag allocation schemes. Note here that before and after the maneuver, the pseudoinverse and minimum drag results coincide. This is because the minimum drag positions for the rudders occur at their minimum deflections. Thus, the pseudoinverse restoring actually results in a minimum drag solution for the rudders when they are not needed. In contrast to the previous figures, however, the rudder deflections during the maneuver for the pseudoinverse restoring are actually larger in magnitude than the minimum drag restoring. This reemphasizes the tradeoff that the minimum drag allocation has made, in this case, between the rudder and aileron yaw and drag characteristics while attempting to allocate

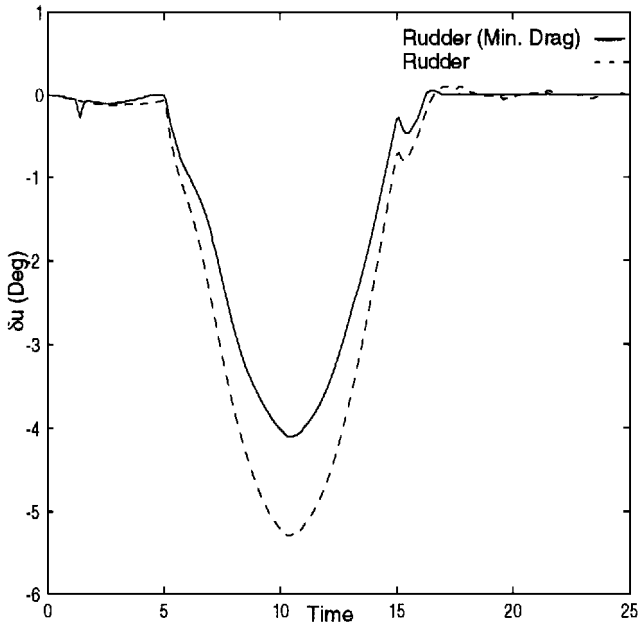

Fig. 5 Rudder time histories.

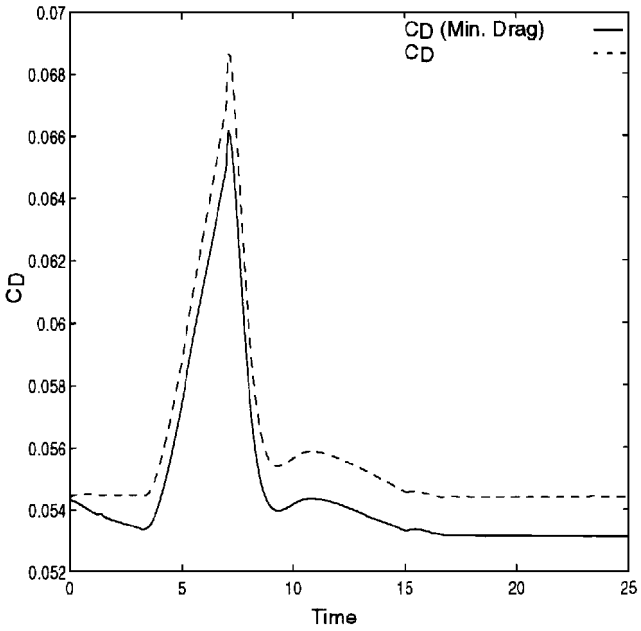

Fig. 6 Drag coefficient time histories.

toward minimum drag. Finally, Fig. 6 compares the drag coefficients for the pseudoinverse and minimum drag allocation schemes during the maneuver. As expected, the minimum drag results are less throughout the entire maneuver. When the steady-state conditions are reached, the control deflections given by the minimum drag allocation scheme result in a 2.4% reduction in drag.

Conclusions

The example has demonstrated that whereas direct control allocation itself presents a powerful approach to solving the three-moment, multiple control problem, it can also be modified, with relative ease, to account for a larger four-objective, multiple control problem. In this case, drag was considered a fourth objective, which the allocator was instructed to minimize. The minimization procedure here is not the usual iterative/optimization algorithm; it simply allocates toward this state. Whether it settles on a minimum drag state or not depends primarily on the tasks that the aircraft is performing. In the case of extended periods of inactivity where the control laws are not demanding extreme control deflections (like trimmed flight), the allocation procedure does in fact achieve a minimum drag configuration.

Acknowledgments

This work was conducted under NASA Research Grant NAG 1-1449 supervised by John V. Foster of the NASA Langley Research Center.

References

[1]Durham, W., and Bordignon, K., "Multiple Control Effector Rate Limiting," *Journal of Guidance, Control, and Dynamics*, Vol. 19, No. 1, 1996, pp. 30–37.

[2]Durham, W. C., "Constrained Control Allocation: Three-Moment Problem," *Journal of Guidance, Control, and Dynamics*, Vol. 17, No. 2, 1994, pp. 330–336.

[3]Durham, W., "Constrained Control Allocation," *Journal of Guidance, Control, and Dynamics*, Vol. 16, No. 4, 1993, pp. 717–725.

[4]Stevens, B., and Lewis, F., *Aircraft Control and Simulation*, Wiley, New York, 1992, pp. 593–602.

Noetherian Perspective of Eulerian Motion of a Free Rigid Body

Yoshihiko Nakamura*
University of Tokyo, Tokyo 113, Japan
and
Ranjan Mukherjee†
Michigan State University, East Lansing, Michigan 48824-1226

Introduction

CONSERVATION laws play an important role in mechanics from both a theoretical and a practical standpoint. They can considerably simplify the integration of the differential equations of motion. Also, they can be regarded as the manifestation of some profound physical principle. Although there are a variety of approaches for finding conservation laws, the most popular and modern method is based on the study of the invariant properties of the Lagrangian with respect to infinitesimal transformations of the generalized coordinates describing the configuration of the system and time. This approach is based on Noether's famous theorem.[1] Noether's theory can be regarded as a generalization of the theory of ignorable coordinates[1] although it is not usually treated from this viewpoint.

There exists a conservation law for conservative scleronomic systems, or for mechanical systems whose Lagrangian functions are not explicit functions of time. This conservation law is identical to the conservation of energy if the kinetic energy of the system can be expressed in a form quadratic in the generalized velocities. The conservation law can be obtained by redefining time as one of the generalized coordinates and using the theory of ignorable coordinates[1] or by applying Noether's theorem after an infinitesimal transformation of time.[1]

It is well known that the linear momentum of a rigid body is a conserved quantity in the absence of external forces. This conservation law can be obtained from the theory of ignorable coordinates[1] by observing that the kinetic energy of the body is not a function of the coordinates of the center of mass. Linear momentum conservation can also be established by using Noether's theorem[1] after an infinitesimal translation of the coordinate system.

The angular momentum of a free rigid body (rigid body in the absence of external forces and moments) is a conserved quantity. If Euler angles are used for the description of orientation of the

Received June 10, 1996; revision received Sept. 30, 1996; accepted for publication Oct. 21, 1996.

*Associate Professor, Department of Mechano-Informatics, 7-3-1 Hongo, Bunkyo-ku.

†Associate Professor, Department of Mechanical Engineering.